ISSN 1063-780X, Plasma Physics Reports, 2015, Vol. 41, No. 10, pp. 814–819. © Pleiades Publishing, Ltd., 2015.
Original Russian Text © I.V. Romadanov, S.V. Ryzhkov, 2015, published in Fizika Plazmy, 2015, Vol. 41, No. 10, pp. 884–889.

PLASMA DYNAMICS

Regimes of Pulsed Formation of a Compact Plasma Configuration with a High Energy Input

I. V. Romadanov and S. V. Ryzhkov

Bauman Moscow State Technical University,
ul. Vtoraya Baumanskaya 5-1, Moscow, 105005 Russia
e-mail: ryzhkov@power.bmstu.ru

Received March 26, 2014; in final form, March 16, 2015

Abstract—Results of experiments on the formation of a compact toroidal magnetic configuration at the Compact Toroid Challenge setup are presented. The experiments were primarily aimed at studying particular formation stages. Two series of experiments, with and without an auxiliary capacitor bank, were conducted. The magnetic field was measured, its time evolution and spatial distribution over the chamber volume were determined, and its influence on the formation regimes was investigated.

DOI: 10.1134/S1063780X15100074

1. INTRODUCTION

The compact torus (CT) is an axisymmetric magnetic configuration for hot plasma confinement, alternative to the tokamak [1–3]. Advantages of this configuration are the purely poloidal magnetic field, the presence of open magnetic field lines and a natural divertor, and the high b value (the ratio of the plasma gas-kinetic pressure to the pressure of the external magnetic field). This configuration may be used for the development of a special type of reactor [4, 5], for tokamak refueling [6], as a neutron source [7], as a magnetized target in the scheme of magnetic–inertial confinement fusion [8, 9], in rocket engines [10, 11], in systems with a liquid wall [12], and in other applications [13]. At present, the following methods for CT generation have been studied well enough: the method based on the θ-pinch [14, 15], the merging of spheromaks [16] and field-reversed configurations (FRCs) [17, 18], the method of a rotating magnetic field [19, 20], and the method employing a central electrode [21]. One of the problems of CT generation is the low level of the trapped magnetic flux and, as a consequence, the low value of the energy transferred from the energy source to the plasma. In [22–25], a method for CT formation was proposed that would allow one to increase the trapped magnetic flux and the energy deposited in the plasma. The method is similar to the θ-pinch method, but has some distinctions. In this work, we present results from experiments on the CT formation by this method with a pulsed energy input to the plasma.

2. SCHEME OF CT FORMATION

In accordance with the discharge of the feeding capacitor banks, several stages can be distinguished in the process of CT formation (Fig. 1).

Stage a. The solenoidal current I_1 is driven, which creates a poloidal magnetic field $\mathbf{B}_p$ in the chamber volume. When the current I_1 reaches its maximum value, it is cut off.

Stage b. The cutoff of the current I_1 leads to the emergence of the azimuthal current I_θ in plasma, which impedes the decrease in the magnetic field due to the mutual induction effect. According to the Lenz law, the azimuthal current I_θ flows in the same direction as the solenoidal current I_1. The azimuthal current I_θ sustains the poloidal magnetic field $\mathbf{B}_p$.

Stage c. Simultaneously with the cutoff of the current I_1, the current I_0 that is larger in magnitude is passed along the chamber axis. The current I_0 generates the azimuthal magnetic field $\mathbf{B}_t$. Since the magnitude of this field is larger than B_p, electrons and ions creating the plasma current move mainly along the force lines of the magnetic field $\mathbf{B}_t$, thereby sustaining the azimuthal current I_θ. A typical particle trajectory is shown in Fig. 2, where the pitch of the helix is increased for clarity, and the axes are in the dimensionless units. The resulting configuration is, in essence, an elongated CT.

Stage d. After the cutoff of the longitudinal current I_0, the solenoidal current I_2 (the largest in magnitude) is switched on to push the plasma away from the chamber walls due to the Ampère force between the current I_2 and the azimuthal current I_θ in plasma.

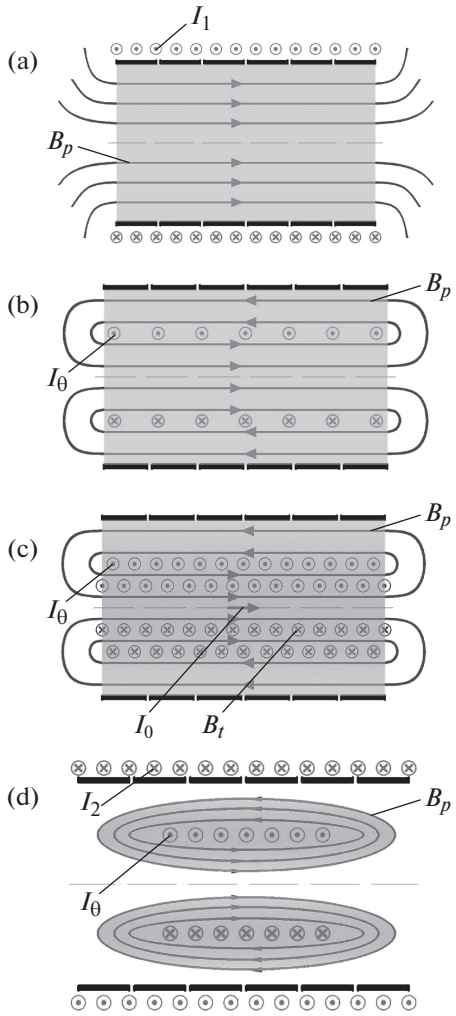

Fig. 1. Different stages of CT formation: (a) the coil current I_1 leads to the generation of the poloidal magnetic field B_p; (b) after the cutoff of the current I_1, the azimuthal current I_θ and the poloidal magnetic field B_p arise in plasma; (c) the current I_0 flowing along the chamber axis creates the toroidal magnetic field B_t; and (d) pushing the plasma away from the chamber walls and its compression under action of the Ampère force.

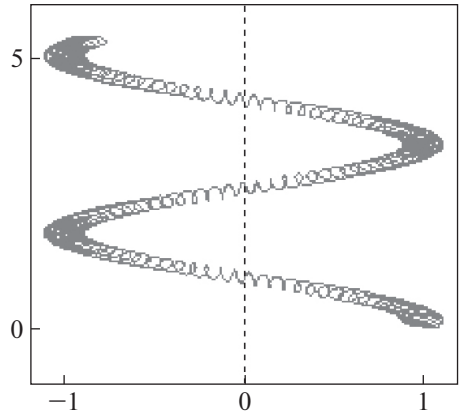

Fig. 2. Typical particle trajectory in the field of the current I_0.

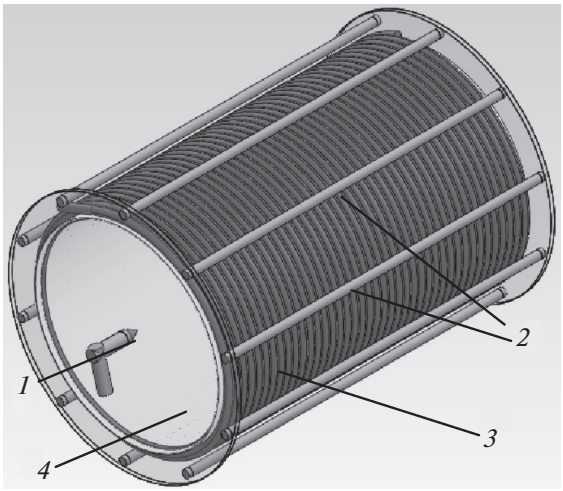

Fig. 3. General view of the vacuum chamber with external electrodes: (*1*) central electrode, (*2*) ten electrodes arranged over the perimeter of the chamber, (*3*) coil, and (*4*) flange.

3. EXPERIMENTAL SETUP

The Compact Toroid Challenge (CTC) setup (Lebedev Physical Institute, Russian Academy of Sciences) [24] is intended to study and develop the proposed method of CT formation. The setup consists of the formation chamber, three independent capacitor banks, a vacuum system, vacuum spark-gaps, and a control system.

A general view of the formation chamber is given in Fig. 3. The chamber is a 0.5-m-diameter 0.85-m-long cylinder, on which the main (49 turns) and auxiliary (48 turns) coils (solenoids) are wound. Each coil is connected to its own galvanically isolated capacitor bank in such a way that the currents in the main and auxiliary coils flow in opposite directions.

To ensure the required values of the current in the corresponding coils, the banks contain different numbers of capacitors: 22 in the main bank, 32 in the longitudinal-current bank, and 42 in the auxiliary bank. During the discharge of the first bank (via a vacuum spark-gap and current switch), the current flows through the main solenoid. The second bank is discharged through the auxiliary coil, which ensures the transverse compression of the configuration. The third bank induces the current I_0 along the chamber axis and the toroidal magnetic field. The capacitance of one capacitor is 5 μF, the total stored energy at a charging voltage of 25 kV is 150 kJ, the maximum magnetic field on the chamber axis is 0.3 T, and the peak current value is 25 kA.

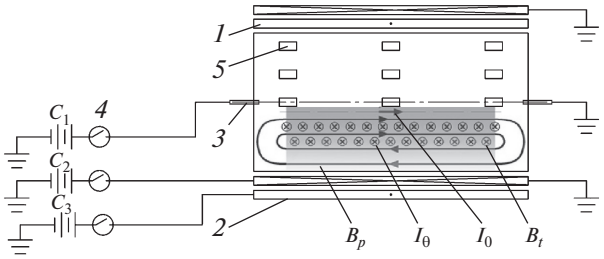

Fig. 4. Block diagram of the CTC setup: (*1*) main solenoid, (*2*) auxiliary solenoid, (*3*) central electrode, (*4*) spark-gaps, (*5*) probes, and (*C1*–*C3*) capacitor banks. Here, B_p is the poloidal magnetic field, B_t is the toroidal magnetic field, I_θ is the toroidal current, and I_0 is the axial current.

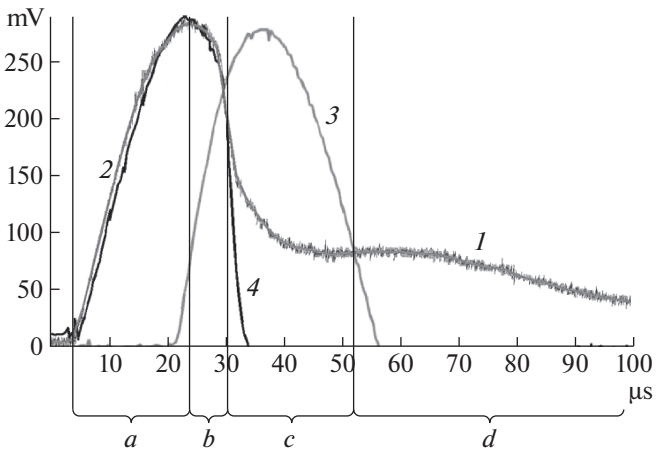

Fig. 5. Diagram of setup operation: (*1*) signal from the detector of the longitudinal magnetic field B_p, (*2*) filtered signal from the detector of the longitudinal magnetic field B_p, (*3*) signal from the detector of the longitudinal current I_0, and (*4*) signal from the detector of the main solenoid current I_1. The designation of the stages is the same as in Fig. 1.

Figure 4 shows the block diagram of the setup and also depicts the final stage of CT formation. Magnetic probes *5* and Rogowski coils (not shown in the figure) were used for measurements. The magnetic probes were arranged on the chamber axis, at the half-radius of the chamber, and near the wall in such a way that the measurements were conducted only along the z axis. The Rogowski coils were installed on the current leads of each capacitor bank. A plasma diagnostic system on the basis of images taken with a high-speed camera was also tested.

Hydrogen was used as a plasma-forming gas. The formation chamber was evacuated using a diffusion oil-vapor vacuum pump. The feeding cables were made of unalloyed copper. The characteristics of the experimental setup are listed in the table.

Figure 5 shows the waveforms of the current passed through the main solenoid (curve *4*) and the longitudinal current flowing through the plasma (curve *3*). Each current was measured using its own voltage divider, and the measured peak current values coincided. The current pulses overlapped in time to ensure the continuity of CT formation; therefore, separation of the entire process of CT formation into stages is rather conventional. It can be seen from Fig. 5 that the current I_0 (unlike the current I_1) is not cut off at the maximum and terminates after one half-period (about 25 μs).

Table 1. Parameters of the discharge circuit and the plasma

Parameter	Value
Initial values	
Coil inductance, nH	4.78
Cable resistance, mΩ	25
Capacitance of one capacitor, μF	5
Spark-gap inductance, nH	100–900
Rate of change in the spark-gap resistance, mΩ/μs	50–250
After discharge	
Plasma inductance L_p, nH	150–800
Plasma resistance R_p, mΩ	180–900

4. EXPERIMENTAL RESULTS

The experiments performed in two regimes of plasma formation with different degrees of preionization have shown that the final plasma parameters depend only on the initial preionization. Preionization is produced by a short discharge of a special capacitor bank and its degree is determined by the charging voltage of the capacitor bank. At a low degree of preionization (less than 5×10^{13} cm^{-3}), the magnetic field rapidly penetrates into the plasma simultaneously with its heating, which results in a final configuration with a low β value (<0.6). At a high degree of preionization (more than 10^{14} cm^{-3}), the time of magnetic field diffusion increases nearly twofold, which results in a configuration with a high β value (>0.6), the peak plasma density being ~10^{15} cm^{-3}. The experimental results presented below were obtained in the second operating regime.

The main objective of our experiments was to study the CT formation regime. For this purpose, the magnetic field, its time evolution, and its distribution over the chamber volume were measured. Figure 6 presents results from two series of experiments in which different stages of CT formation were studied. The first series consisted of four successive discharges, while the second consisted of two discharges. The experiments were conducted with and without an auxiliary capacitor bank.

The magnetic field near the wall (Fig. 6, curves *1*) changes its sign, while the magnetic field at the half-radius (Figs. 6, curves *3*) drops almost to zero. At the same time, the magnetic field on the chamber axis (Figs. 6, curves *2*) does not change its sign, which indicated the formation of an FRC.

A considerable decrease in the magnetic field on the chamber axis (Fig. 6b, curves *2*) is related to the problem of synchronization of the cutoff of the current I_1 with the switching-on of the longitudinal current I_0, i.e., in fact, to the difficulty in determining the time of current termination in the main solenoid due to the insufficient speed of current switches. It is important to synchronize currents in such a way that the longitudinal current be switched on simultaneously with the cutoff of the main currents. Measurements of the currents flowing through the solenoids made it possible to check this synchronization. Nevertheless, when the I_2 current was passed through the auxiliary solenoid, the magnetic field on the chamber axis increased (Fig. 6b, curves *2*) due to an increase in the plasma current and a decrease in the configuration dimensions.

Using different experiment schemes, it is possible to vary the configuration lifetime and the level of the trapped magnetic flux, as well as to observe the behavior of the configuration under these conditions. Plasma self-heating and an increase in magnetic flux due to configuration pinching (maxima of curves *1* and *2* in Fig. 6) also play an important role. These effects allow one to increase the plasma lifetime and final plasma temperature. Further experiments should be aimed at combining different methods for enhancing the efficiency of the process and increasing the plasma lifetime and final plasma temperature. The reported experiments were not aimed at measuring the full lifetime of the configuration, but were focused on the development of the CT formation method.

Figure 7a shows the level of the trapped magnetic flux in experiments carried out by Kurtmullaev et al. [26]. It can be seen from the figure that the trapped magnetic flux is on the order of 50% (the peak is related to the current maximum in the first stage, before the reverse coil is switched on). In other experiments, this parameter was at a level of 20–30%.

Due to the cutoff of the current in the main solenoid and the use of the longitudinal current and the auxiliary capacitor bank, it is possible to generate a CT with an increased energy input. In our experiments, the level of the magnetic flux trapped by the plasma reaches 60–70% (see Fig. 7b). The level of the trapped magnetic flux drops abruptly after it reaches its peak value and the current is cut off. If no additional means are applied to sustain the trapped magnetic flux (such as switching-on of the reverse coil), then it decreases gradually. It is worth noting that the experimental technique was far from being ideal and even higher values of the trapped flux were achieved in some series of experiments. The process as a whole resembles the pinching of a wide closed current loop. In contrast to the conventional linear pinch, a great amount of magnetic energy can be stored in such a loop, as is in the case of a single-turn inductive energy storage.

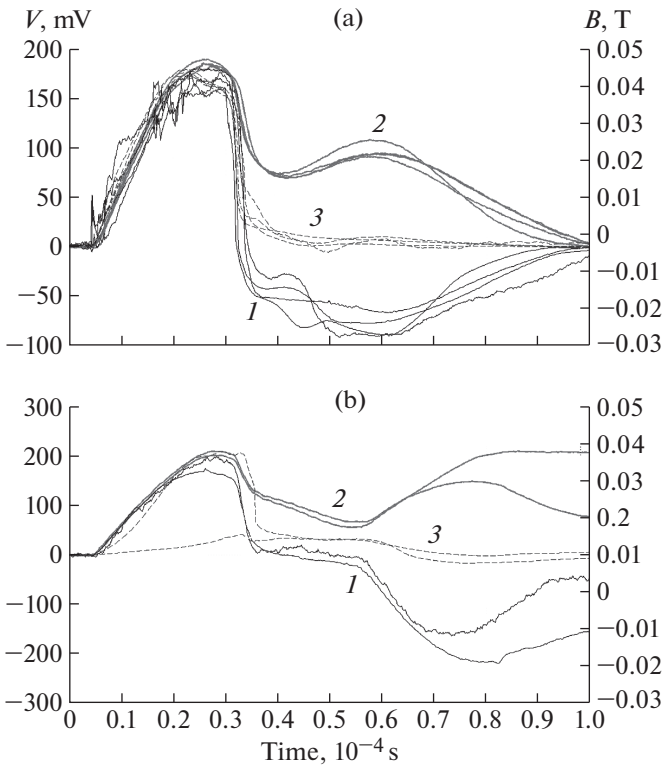

Fig. 6. Time dependences of the magnetic field B_p measured (a) in a series of four discharges with the use of an auxiliary capacitor bank and (b) in two discharges without an auxiliary capacitor bank: (*1*) magnetic field near the chamber wall, (2) magnetic field on the chamber axis, and (*3*) magnetic field at the half-radius of the chamber (12.5 cm).

5. PLASMA DIAGNOSTICS BASED ON THE IMAGE PROCESSING

Modern high-speed cameras may be used for diagnostics of different fast processes. Such systems are used at stellarators and tokamaks [27–30]. This method has several advantages, the most important of which is the possibility to obtain a two-dimensional picture of the process in real time. A series of such images allows one to investigate the plasma inhomogeneity. On the other hand, processing of these images may provide information on the plasma parameters. A plasma diagnostic system on the basis of images taken with a high-speed camera was tested in our experiment by means of calibration of the image intensity in accordance with the known plasma parameters measured by other methods (e.g., by spectroscopy). In the course of the experiment, plasma images were taken synchronously with passage of the current, which

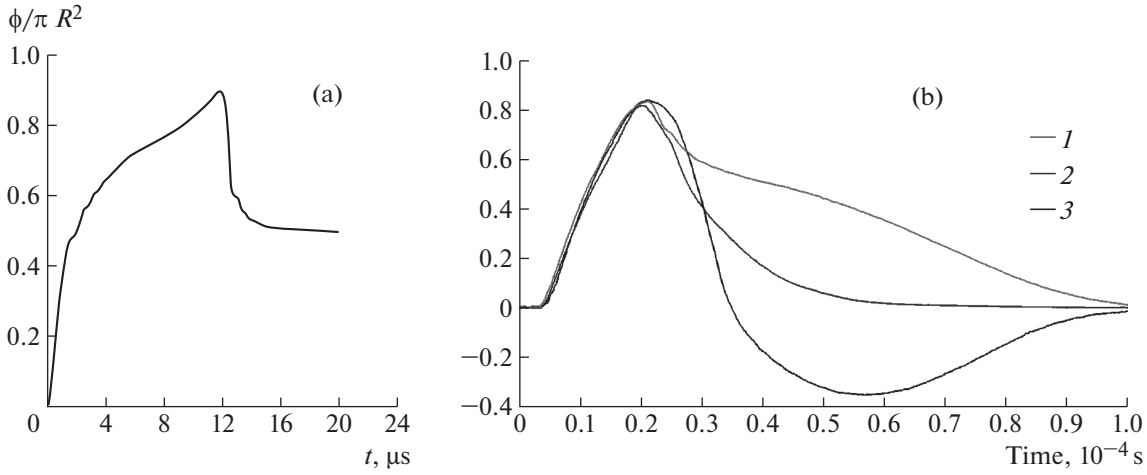

Fig. 7. Comparison of the levels of the trapped magnetic flux obtained (a) by Kurtmullaev et al. [26] and (b) at the CTC setup: (*1*) magnetic field on the chamber axis, (*2*) magnetic field at the half-radius of the chamber (12.5 cm), and (*3*) magnetic field on the chamber wall.

allowed us to increase the resolution and obtain a more detailed picture of the experiment.

Figure 8 shows the distribution of the plasma temperature and the ring structure of the current sheet. These data agree with the results of magnetic probe measurements of the CT formation. The presented picture is obtained by eliminating noise by means of a two-dimensional median filter and the subsequent smoothing by a Gaussian filter. The temperature is determined from the intensity of the initial image by using precalibrated intensity values. To avoid the preionization effect, the images were taken without a magnetic field.

6. CONCLUSIONS

Several series of experiments on the formation of CT magnetic configurations with different plasma parameters were carried out at the CTC setup. The main task was to confirm the method for CT formation and study different formation stages. Results from two series of experiments with and without the auxiliary capacitor bank are presented. In the course of the experiment, the magnetic field, its time evolution, and its distribution over the chamber volume were measured. Measurements of the currents flowing through different solenoids made it possible to achieve their synchronization.

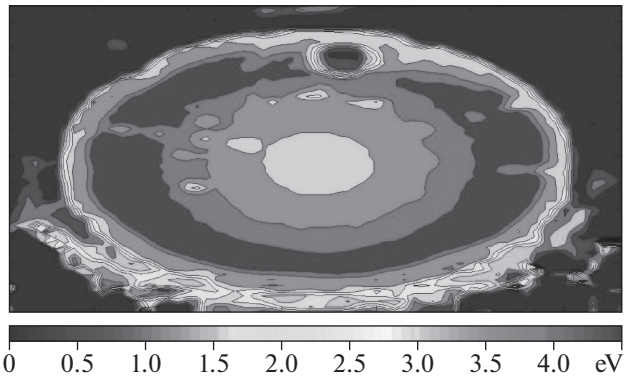

Fig. 8. Spatial distribution of the plasma temperature over the chamber volume.

The use of different experimental schemes allows one to increase the configuration lifetime and the level of the trapped magnetic flux. Other important effects are plasma self-heating and an increase in the magnetic flux due to configuration pinching.

This study was aimed at verifying the proposed method of CT formation and was not intended to consider in detail plasma processes. In our experiments, we succeeded to obtain a CT configuration that existed for a fairly long time. In this stage, we did not consider the influence of plasma instabilities on the process of CT formation. These issues are undoubtedly important and will be explored in our further studies.

ACKNOWLEDGMENTS

We are grateful to A.G. Mozgovoy for his optimism, the naming of the setup, and his assistance in this work. This work was supported by the Ministry of Education and Science of the Russian Federation, state contract no. 13.79.2014/K.

REFERENCES

1. G. I. Dudnikova, R. Kh. Kurtmullaev, A. I. Malyutin, and V. N. Semenov, Sov. J. Plasma Phys. **15**, 572 (1989).
2. L. C. Steinhauer, Phys. Plasmas **18**, 070501 (2011).

3. S. V. Ryzhkov, Plasma Phys. Rep **37**, 1075 (2011).
4. N. Rostoker, M. W. Binderbauer, and H. J. Monkhorst, Science **278**, 1419 (1997).
5. S. V. Ryzhkov, V. I. Khvesyuk, and A. A. Ivanov, Fusion Sci. Technol. **43** (1T), 304 (2003).
6. A. L. Hoffman, P. Gurevich, J. Grossnickle, and J. T. Slough, Fusion Technol. **36**, 109 (1999).
7. J. Slough, Fusion Sci. Technol. **60**, 464 (2011).
8. S. V. Ryzhkov, Bull. Russ. Acad. Sci. **78**, 456 (2014).
9. A. Yu. Chirkov and S. V. Ryzhkov, J. Fusion Energy **31** ((1)), 7 (2012).
10. S. V. Ryzhkov, Fusion Sci. Technol. **47** (1T), 342 (2005).
11. J. Slough, D. Kirtley, A. Pancotti, M. Pfaff, C. Phil, and G. Votroubek, in *Proceedings of the 39th IEEE International Conference on Plasma Science, Edinburgh, 2012,* Paper 1P-125.
12. R. W. Moir, R. H. Bulmer, K. Gulec, P. Fogarty, B. Nelson, M. Ohnishi, M. Rensink, T. D. Roghlien, J. T. Santarius, and D. K. Sze, Fusion Technol. **39**, 758 (2001).
13. S. V. Ryzhkov, in *Proceedings of the 35th EPS Conference on Plasma Physics, Hersonissos, 2008,* ECA **32D**, 561 (2008).
14. M. I. Kutuzov, V. N. Semenov, and V. F. Strizhov, Sov. J. Plasma Phys. **7**, 520 (1981).
15. M. Tuszewski, Nucl. Fusion **28**, 2033 (1988).
16. C. D. Cothran, A. Falk, A. Fefferman, M. Landreman, M. R. Brown, and M. J. Schaffer, Phys. Plasmas **10**, 1748 (2003).
17. J. Slough, G. Votroubek, and C. Pihl, Nucl. Fusion **51**, 053008 (2011).
18. H. Guo, M. Binderbauer, and D. Barnes, Phys. Plasmas **18**, 056110 (2011).
19. A. L. Hoffman, Phys. Plasmas **5**, 979 (1998).
20. M. Inomoto, K. Kitano, and S. Okada, Phys. Rev. Lett. **99**, 175003 (2007).
21. C. S. Niemela and L. B. King, in *Proceedings of the 31st International Electric Propulsion Conference, Ann Arbor*, 2009, Paper IEPC-2009-008.
22. I. V. Romadanov, Nauka Obrazov., No. 2 (2012), http://technomag.bmstu.ru/file/out/505114
23. I. V. Romadanov, Probl. At. Sci. Technol., No. 1, 39 (2013).
24. A. G. Mozgovoy, I. V. Romadanov, and S. V. Ryzhkov, Phys. Plasmas **21**, 022501 (2014).
25. I. V. Romadanov and S. V. Ryzhkov, Fusion Eng. Des . **89**, 3005 (2014).
26. R. Kh. Kurtmullaev, A. I. Malyutin, and V. N. Semenov, in *Advances in Science and Technology, Ser. Plasma Physics,* Ed. by V. D. Shafranov (VINITI, Moscow, 1985), Vol. 7, p. 80 [in Russian].
27. O. Chumak and M. Hrabovský, Czech. J. Phys. **56**, B767 (2006).
28. J. A. Grossnickle, R. D. Brooks, C. L. Deards, A. L. Hoffman, P. A. Melnik, K. E. Miller, R. D. Milroy, K. M. Velas, G. C. Vlases, and the RPPL Team, J. Fusion Energy **29**, 517 (2010).
29. E. De la Cal, J. Guasp, and the TJ-II Team, Plasma Phys. Controlled Fusion **53**, 085006 (2011).
30. Y. Sechrest, T. Munsat, D. A. D'Ippolito, R. J. Maqueda, J. R. Myra, D. Russell, and S. J. Zweben, Phys. Plasmas **18**, 012502 (2011).

Translated by M. Samokhina

SPELL: OK